



Beyond the Promoter: Total *MGMT* Gene Methylation Modulates Response to DNA-Alkylating Agents in Glioma

Nicole J. Briceno^{1,2}, Jinkyu Jung¹, Aiguo Li¹, Chunzhang Yang¹, Mioara Larion¹, Lorinc S. Pongor³, Fathi Elloumi³, Sudhir Varma³, William C. Reinhold³, Yves Pommier³, Mark R. Gilbert¹, and Orieta Celiku^{1,4}

ABSTRACT

Patients with malignant gliomas with methylated *MGMT* promoters are generally more sensitive to alkylating chemotherapy as this modification impedes DNA repair. However, inconsistencies in the predictive accuracy of *MGMT* promoter methylation have been observed. We hypothesize that these variations may be partially explained by a counteracting influence of *MGMT* gene body methylation. Data from The Cancer Genome Atlas were analyzed to assess correlations between *MGMT* promoter and body methylation with transcript production across cancer types and within glioma subcohorts. Thirty-six human glioma cell lines underwent molecular profiling via Illumina 850k Methylation Arrays and RNA sequencing. A subset was further tested for *MGMT* protein levels and carmustine response. Correlations and linear regression analyses were conducted to investigate association of carmustine sensitivity with different levels of *MGMT* expression. *MGMT*

mRNA expression was positively correlated with body methylation and negatively correlated with promoter methylation across cancers from The Cancer Genome Atlas. Body and promoter methylation were anticorrelated in the non-glioma cohort and *IDH1/2* wild-type glioma subcohort but not correlated in the *IDH1/2*-mutated subcohort. Most glioma cell lines did not express *MGMT* mRNA. In the cell lines tested for carmustine response, sensitivity was negatively correlated with body methylation and mRNA expression and positively correlated with promoter methylation. Our findings further expound the relationship between *MGMT* methylation patterns and alkylating agent response, with body methylation playing a significant role. The identified role of gene body methylation underscores the need to integrate the interplay between promoter and body methylation in clinical testing and predicting treatment outcomes.

Introduction

There are a limited number of effective treatment regimens for patients with malignant gliomas. The current standard of care consists of surgery followed by chemotherapy and/or radiation. Common chemotherapies are nitrosoureas, such as lomustine or carmustine, or the imidazotetrazine temozolomide. These agents alkylate purine residues, particularly O⁶ guanine, causing inter-strand cross-links that damage DNA, block replication, and lead to cell death (1, 2).

To determine whether chemotherapy with alkylating agents is an appropriate treatment, gliomas are tested to assess the promoter methylation status of *MGMT* (O⁶-methylguanine-DNA methyltransferase). *MGMT* is an enzyme that repairs guanine residues by sequestering the O⁶ methyl from the damaged purine site, a process

that irreversibly inactivates the enzyme and necessitates *de novo* protein synthesis to maintain enzyme activity (3). The expression of *MGMT* is largely controlled by gene promoter methylation, with hypermethylation of the promoter suppressing *MGMT* expression and conferring an improved response to alkylating agents (4, 5). Yet, not all patients with *MGMT* promoter hypermethylation respond to these therapies or have durable response (6–8). Methods of methylation detection, the DNA sites tested, and cutoffs used as thresholds for positive methylation status vary and have resulted in differing detection and call levels (9, 10), which may contribute to some discrepancies.

In small cell lung cancer, methylation profiling as it relates to drug treatment response identified methylation status of the gene body as well as other non-promoter regions to be predictive of response (6, 11). Among multiple cancer types, gene body hypermethylation has been associated with gene overexpression, tumor invasion, and progression (12, 13). Moreover, interactive exploration of sarcoma cell line data from CellMinerCDB suggests that *MGMT* mRNA expression is associated with both promoter and body methylation (14, 15). We, therefore, hypothesized that although some of the unexpected outcomes to DNA-alkylating agents may be reflective of the technology used to determine the *MGMT* promoter methylation status, methylation of the *MGMT* body is an important component of the resulting expression and has significant clinical implications (Fig. 1). To elucidate this relationship in the context of glioma, we examined the implications of *MGMT* gene promoter and body methylation levels on *MGMT* mRNA expression across The Cancer Genome Atlas (TCGA) cohort, as well as on a panel of human glioma cell line models. A subset of the cell line panels was tested to determine response to carmustine treatment and assayed for protein production. We then investigated whether response was associated with different levels of *MGMT* regulation.

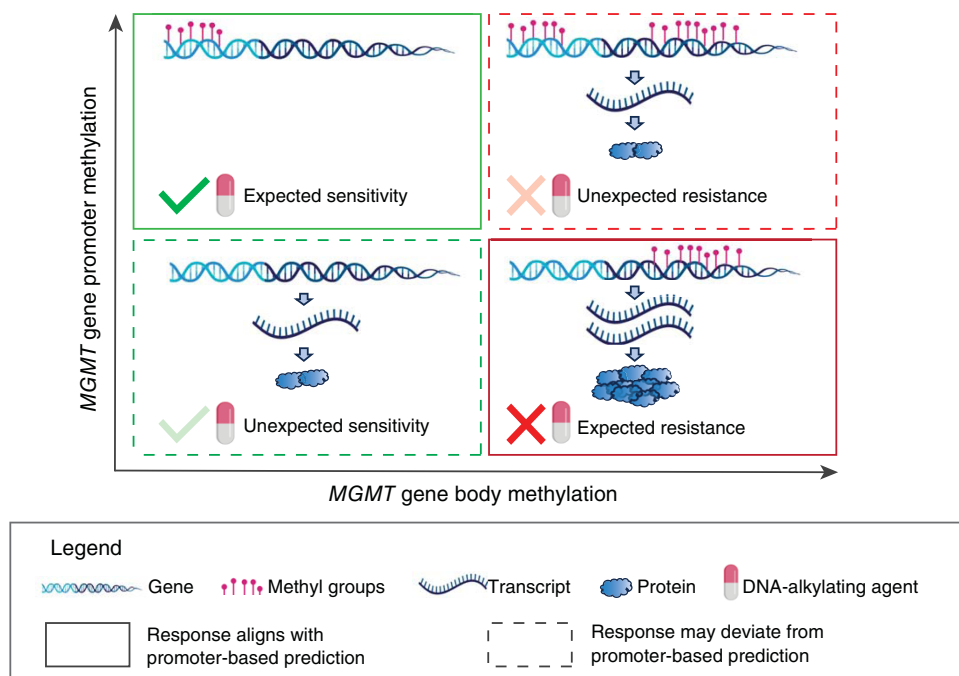
¹Neuro-Oncology Branch, Center for Cancer Research, National Cancer Institute, National Institutes of Health, Bethesda, Maryland. ²Prenatal Genomics and Therapy Section, Center for Precision Health Research, National Human Genome Research Institute, National Institutes of Health, Bethesda, Maryland. ³Laboratory of Molecular Pharmacology & Genomics and Pharmacology Facility, Developmental Therapeutics Branch, Center for Cancer Research, National Cancer Institute, National Institutes of Health, Bethesda, Maryland. ⁴IT Services and Support Branch, Center for Biomedical Informatics & Information Technology, National Cancer Institute, National Institutes of Health, Rockville, Maryland.

Corresponding Author: Orieta Celiku, IT Services and Support Branch, Center for Biomedical Informatics & Information Technology, National Cancer Institute, National Institutes of Health, 9609 Medical Center Drive, Rockville, MD 20850. E-mail: orieta.celiku@nih.gov

Mol Cancer Ther 2025;XX:XX-XX

doi: 10.1158/1535-7163.MCT-24-0977

©2025 American Association for Cancer Research

**Figure 1.**

Response to DNA-alkylating agents depends on MGMT production, influenced by both promoter and body methylation. Promoter hypermethylation typically leads to no MGMT and strong response, whereas the opposite results in high MGMT and resistance. However, in cases between these extremes, predicting response is more challenging. For example, promoter hypomethylation with body hypomethylation may cause low MGMT and unexpected sensitivity, whereas promoter hypermethylation with body hypermethylation can still produce enough MGMT for resistance. This approach refines current prediction models that rely solely on promoter methylation, addressing situations of unexpected resistance or sensitivity. (Partially created using BioRender.com.)

Materials and Methods

Cell lines and cell culture

All cell media were supplemented with 1% antibiotic–antimycotic (Gibco, #15240062), 1% penicillin–streptomycin (Gibco, #15140122), and 250 µg amphotericin B (Gibco, #15290026); cell lines were grown at 37°C in 5% CO₂.

U251 (RRID: CVCL_A5HR) was grown in DMEM (Gibco, #11960044) with 10% FBS and 2 mmol/L L-glutamine (Gibco, #A2916801). Normal human astrocytes (NHA; provided by Dr. Russell Pieper, RRID: CVCL E3G5) was grown in complete astrocyte media (ScienCell, #1801) with 10% FBS and 1% astrocyte growth supplement. GSC923, GSC827 (16), GSC274 (provided by Dr. Erik Sulman), and XO10 were grown in neurobasal media (NBM; Gibco, #21103049) with 1 mmol/L sodium pyruvate (Gibco, #11360070), 1× B27 without vitamin A (Gibco, #12587010), 1× N2 (Gibco, #17502001), 20 ng/mL epidermal growth factor (EGF) (Fujifilm Irvine Scientific, #100-26), and 20 ng/mL fibroblast growth factor (FGF)-basic (154aa; Fujifilm Irvine Scientific, #100-146). MGG119 (provided by Dr. Andrew Chi; ref. 17) and GSC403 media included 1:1 DMEM/F12 (Gibco, #11320033) to NBM with 1× GlutaMAX (Gibco, #35050061) and 25 ng/mL EGF and FGF-basic (154aa). TS603 (provided by Dr. Timothy Chan, RRID: CVCL_A5HW) was grown in DMEM/F12 media supplemented with 1× N2, 1 mg heparin (STEMCELL Technologies, #07980), and 25 ng/mL EGF and FGF-basic (154aa). DIPG17 (provided by Dr. Michelle Monje, RRID: CVCL_C1MW) was grown in 1:1 NBM:DMEM/F12, 1 mmol/L sodium pyruvate, 100 mmol/L minimum essential medium nonessential amino acids solution (Gibco, #11140050), 1× GlutaMAX, 10 mmol/L HEPES solution (Gibco, #15630080), 1× B27 without vitamin A, 20 ng/mL EGF and FGF, 10 ng/mL platelet-derived growth factor-AA (PDGF-AA) (Fujifilm Irvine Scientific, #100-16) and PVDF-BB (Fujifilm Irvine Scientific, cat. #100-18), and 1 mg heparin. GSC923, GSC827, GSC403, and XO10 cell lines were established by the NCI Neuro-Oncology Branch.

GSC827, GSC923, U251, NHA, and TS603 were tested for *Mycoplasma* by NCI Frederick using the MycoAlert Mycoplasma Detection Kit (Lonza, LT07-318). NHA, GSC923, DIPG17, GSC274, and MGG119 were cultured up to 10 passages, GSC403 up to eight passages, and TS603 up to 15 passages. Cells were split every 48 to 72 hours with supplemental feeding at 24 hours after passage.

Cell line cultures were monitored by microscopy. DNA sequencing and methylation signature classification were used for authentication.

RNA sequencing

Total RNA was isolated from cell pellets using the Qiagen RNeasy Mini kit, with a DNase digest step performed on the QIAcube, and quantified with Qubit Broad-Range RNA kit (Invitrogen, #Q10210), and RNA integrity number was calculated through Agilent Bioanalyzer (RRID: SCR_018043). RNA samples were pooled and sequenced on NovaSeq S2 using the Illumina TruSeq Stranded mRNA Library Prep Kit and paired-end sequencing. All samples had 48 to 101 million pass filter reads with more than 90% of bases above the quality score of Q30. Reads were trimmed to remove adapters and low-quality bases using Cutadapt (RRID: SCR_011841) and subsequently aligned with the reference genome (human hg38) using CCBP Pipeliner (18).

DNA methylation profiling and classification

DNA was isolated from cell pellets using the Qiagen DNeasy Blood and Tissue kit (Qiagen, #69504) and Zymo Clean and Concentrator-25 kit (Zymo Research, #D4033). Quantity was determined using the Qubit 1× dsDNA High Sensitivity kit (Invitrogen, #Q32854) and 260:280 on NanoDrop 8000 (RRID: SCR_018600). Genome-scale DNA methylation was profiled using the Illumina Human Infinium Methylation EPIC BeadChip array according to the manufacturer's instructions. Raw fluorescence signal intensity values were normalized using functional normalization methods

(PreprocessFunnorm) in the minifi R package (19). Normalized mean methylated (M) and unmethylated (U) intensities for each locus were used to calculate β values per sample as $\beta = (M)/(U + M + 100)$. A total of 207 probes fell under the *MGMT* region as annotated by the array manufacturer; two probes with a median P value > 0.01 across samples were filtered out. The β values of 12 promoter-associated probes that fell in CpG islands were averaged to obtain promoter methylation level at the sample level; the β values of 188 probes that were not promoter associated were averaged to obtain body methylation level at the sample level.

Raw methylation data were submitted to the Molecular Neuro-pathology classifier (20) to obtain sample methylation class, chromosomal location copy-number variations, and *MGMT* promoter methylation status using the STP-27 method (21).

Carmustine IC₅₀ determination

Carmustine (BCNU, Sigma-Aldrich, #C0400) was dissolved in 100% ethanol to 100 mmol/L stock concentration. Four replicates for each cell line at optimal passage were plated in quadruplet at a density of 2,500 cells per 100 μ L media for adherent cells and 5,000 cells per 50 μ L for suspension cells. A gradient of 0, 25, 50, 100, or 200 μ mol/L carmustine was prepared at 2 \times for suspension cells and 1 \times for adherent cells. Ethanol was added to make the final concentration in each treatment equal. Either 50 μ L (suspension) or 100 μ L (adherent, previous media removed) was added to the plates and then incubated for 48 hours at 37°C and 5% CO₂. The plates were allowed to equilibrate for 30 minutes at room temperature and then 50 μ L of CellTiter-Glo reagent (Promega, #7571) was added to each well. The plates were covered in foil and gently rocked for 1 hour. Luminescence was read on BMG Labtech POLARstar Optima. IC₅₀ was determined using the absolute IC₅₀ analysis on GraphPad Prism (RRID: SCR_002798).

Protein quantification

For the passage assay, cells were grown to an early (P5 and P3 for GSC403), middle (P8 and P5 for GSC403 and P10 for TS603), and late passage (P10 and P8 for GSC403 and P15 for TS603). For the timed assay, the cells were treated with IC₅₀ of carmustine for each line for 0, 24, 48, or 72 hours. For the concentration assay, the cells were treated with 0, 25, 50, 100, or 200 μ mol/L carmustine for 48 hours.

Western blots were used for protein visualization and quantification. Aliquots of 3×10^6 cells were lysed in RIPA buffer (Thermo Fisher Scientific, #89901) with 1 \times Halt protease inhibitor (Thermo Fisher Scientific, #78425). Total protein was quantified using the DC protein assay kit (Bio-Rad, #5000111) on BioTek Epoch. Gel electrophoresis of 15 μ g of sample was performed using 10% Bis-Tris gels (Thermo Fisher Scientific, #NW00100BOX) and then transferred to a 0.2- μ m polyvinylidene difluoride membrane (Thermo Fisher Scientific, #LC2002). Blots were probed with primary antibodies for *MGMT* (MT3.1, Santa Cruz Biotechnology, #sc56157, RRID: AB_784509; F-5, Santa Cruz Biotechnology, #sc271155, RRID: AB_10614670) at 1:100 or GAPDH (Santa Cruz Biotechnology, #ab181602, RRID: AB_2630358) at 1:60,000 in 2.5% blocking buffer (Bio-Rad, #1706404). After washing in PBS with 0.1% Tween 20 (Thermo Fisher Scientific, #J20605.AP), the blots were incubated in secondary antibodies horseradish peroxidase-conjugated anti-mouse IgG (Cell Signaling Technology, #7076, RRID: AB_330924) at 1:1,000 and horseradish peroxidase-conjugated anti-rabbit IgG (Jackson ImmunoResearch Laboratories Inc., #711-035-152, RRID: AB_10015282) at 1:60,000. Enhanced chemiluminescence

substrate (Bio-Rad, #1705060S) was used to visualize protein and quantified using ImageJ (RRID: SCR_003070).

TCGA data

Pan-cancer data were obtained from the Xena platform (RRID: SCR_018938), including Illumina 450k Methylation Array β values, batch-normalized RNA sequencing mRNA expression, gene-level non-silent somatic mutations, and curated clinical data (22). The dataset comprised 7,588 samples with both methylation and mRNA data with 7,044 non-glioma samples and 544 glioma samples, of which 409 were *IDH1/2* mutated and 135 were *IDH1/2* wild type. A total of 145 (of 175 probes from the *MGMT* region as annotated by the array manufacturer) passed preprocessing and filtering steps as specified in the Xena platform. The β values of nine promoter-associated probes that fell in CpG islands were averaged to obtain promoter methylation level at the sample level; the β values of 132 probes that were not promoter associated were averaged to obtain body methylation level at the sample level.

Statistical analyses

Pearson correlations were used to evaluate associations between *MGMT* promoter and body methylation and other regulatory levels, including mRNA expression, and for a subset of cell lines, protein expression and sensitivity to carmustine. Linear regression models assessed the combined effects of promoter and body methylation on mRNA expression, protein expression, and carmustine IC₅₀, with and without interaction terms. Passage-, time-, and dose-dependent protein expression changes were analyzed using ANOVA. All analyses and visualizations were performed in R (23) utilizing stats, rstatix, ggplot2, ggpubr, and ComplexHeatmap.

Data availability

Data and associated analysis code are available on GitHub (<https://github.com/oricel/MGMT>).

Patient study statement

This study utilized public, de-identified patient data from TCGA, which were collected and utilized following strict human subjects protection guidelines, informed consent, and Institutional Review Board protocols (<https://www.cancer.gov/ccg/research/genome-sequencing/tcga>).

Results

MGMT promoter and body methylation in a pan-cancer cohort

We began by investigating variations in methylation of different *MGMT* regions – promoter and body – across cancers using 7,588 TCGA samples. Focusing on highly diverse samples, **Fig. 2A** shows broad clustering based on methylation similarity in the promoter and body regions. The heatmaps reveal variability by the tissue of origin, region, and specific methylation probe site. Notably, the two glioma cohorts, lower-grade glioma and glioblastoma (GBM), cluster closely despite differences in tumor biology. They also largely align with lymphoid neoplasm diffuse large B-cell lymphoma in both body and promoter; they align with pheochromocytoma and paraganglioma, testicular germ cell tumor, and skin cutaneous melanoma in body methylation. Colorectal adenocarcinoma, despite *MGMT*'s known association with disease progression and response to treatment (24), did not cluster with glioma methylation patterns.

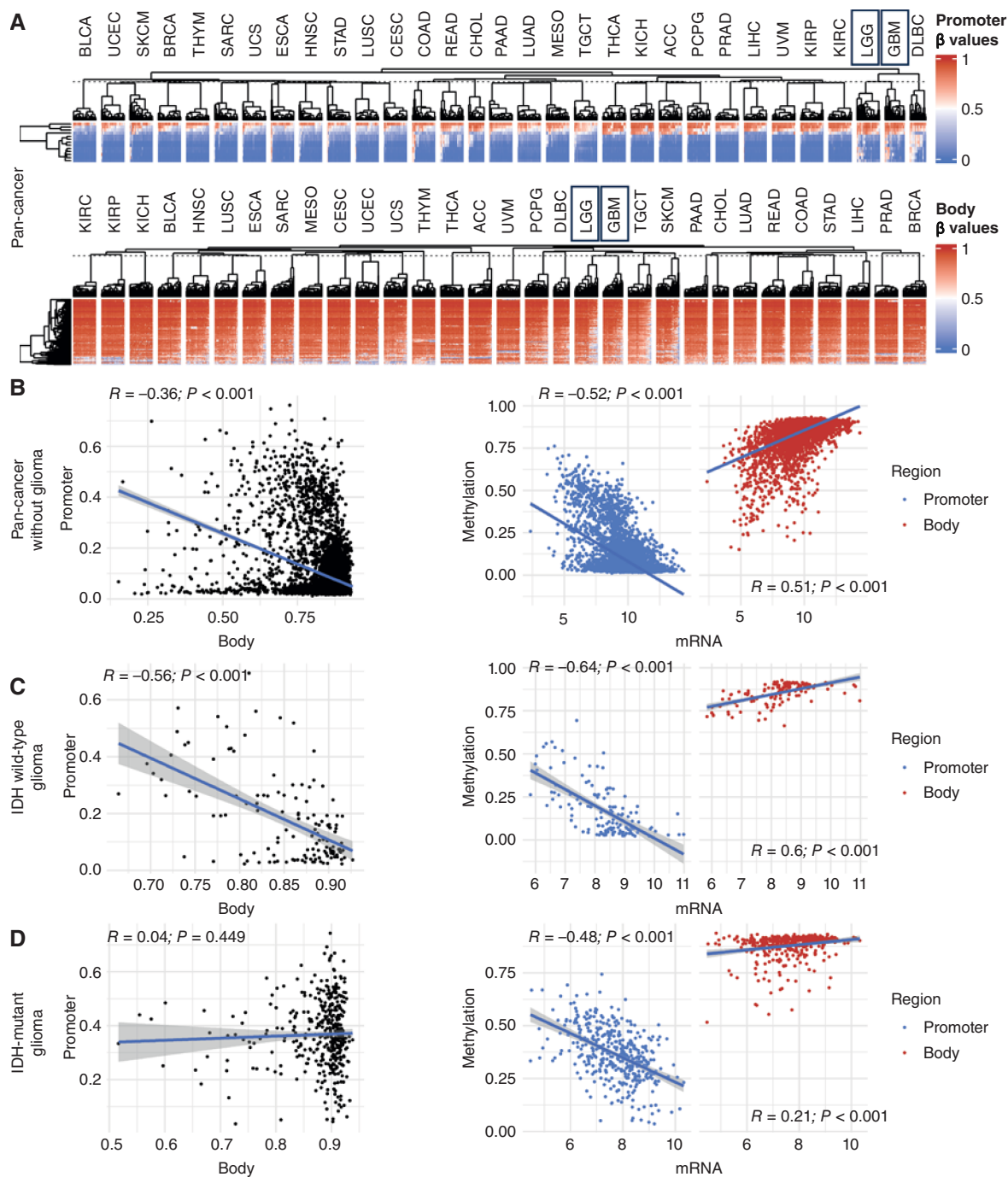


Figure 2.

Methylation of *MGMT* promoter and body across cancer types from TCGA. **A**, Methylation patterns in the full pan-cancer cohort, focusing on the most variable samples (among those within 95% of SD) across each cancer type, with lower-grade glioma (LGG) and glioblastoma (GBM) marked. Rows represent individual probes in the corresponding *MGMT* regions. ACC, adrenocortical carcinoma; BLCA, bladder urothelial carcinoma; BRCA, breast invasive carcinoma; CESC, cervical and endocervical cancers; CHOL, cholangiocarcinoma; COAD, colorectal adenocarcinoma; DLBC, lymphoid neoplasm diffuse large B-cell lymphoma; ESCA, esophageal carcinoma; HNSC, head and neck squamous cell carcinoma; KICH, kidney chromophobe; KIRC, kidney renal clear cell carcinoma; KIRP, kidney renal papillary cell carcinoma; LAML, acute myeloid leukemia; LIHC, liver hepatocellular carcinoma; LUAD, lung adenocarcinoma; LUSC, lung squamous cell carcinoma; MESO, mesothelioma; OV, ovarian serous cystadenocarcinoma; PAAD, pancreatic adenocarcinoma; PCPG, pheochromocytoma and paraganglioma; PRAD, prostate adenocarcinoma; READ, rectum adenocarcinoma; SARC, sarcoma; SKCM, skin cutaneous melanoma; STAD, stomach adenocarcinoma; TGCT, testicular germ cell tumors; THCA, thyroid carcinoma; THYM, thymoma; UCEC, uterine corpus endometrial carcinoma; UCS, uterine carcinosarcoma; UVM, uveal melanoma. **B**, Correlations between promoter and body methylation levels (aggregated by sample) and their correlations with *MGMT* transcription levels in the pan-cancer cohort, excluding glioma. **C**, Correlation data for molecular GBM (*IDH1/2* wild-type glioma). **D**, Correlation data for *IDH1/2*-mutant glioma.

Next, we analyzed methylation correlations by region and their association with mRNA expression, stratifying the glioma cohort by *IDH1/2* mutation status (Fig. 2C and D) and analyzing the non-glioma cohort separately (Fig. 2B). Promoter and body methylation were negatively correlated in the non-glioma cohort ($R = -0.36$; $P < 0.001$) and *IDH1/2* wild-type gliomas ($R = -0.56$; $P < 0.001$) but not correlated in *IDH1/2*-mutant gliomas ($R = 0.04$; $P = 0.499$). mRNA expression was negatively correlated with promoter methylation and positively correlated with body methylation across all cohorts ($P < 0.001$). Linear regression showed significant contributions from both promoter and body methylation in all cohorts (promoter $\beta < 0$; $P < 0.001$ and body $\beta > 0$; $P < 0.001$). Including an interaction term explained additional mRNA expression variance in the non-glioma cohort (interaction $P = 0.003$) but not in the glioma cohorts (interaction $P > 0.05$, Supplementary Table S1).

MGMT promoter and body methylation in a glioma cell line panel

A panel of 36 glioma cell lines and NHAs, including 12 *IDH1* (*IDH*)-mutated lines, was used as a starting point to assess response to alkylating agents (Supplementary Table S2). The panel underwent RNA sequencing, whole-exome sequencing, and methylation profiling via Illumina 850K Methylation Array and was compared with known brain tumor subtypes using the Molecular Neuropathology classifier (20).

As for TCGA dataset analysis, we assessed region-specific *MGMT* methylation patterns, correlations between promoter and body methylation, and their relationship with mRNA expression (Fig. 3). Most cell lines did not express detectable *MGMT* mRNA. The majority displayed high methylation levels across both promoter and gene body regions, with some variability in a subset of probes.

Promoter and body methylation were inversely correlated in *IDH* wild-type lines ($R = -0.58$; $P = 0.003$) but showed no significant correlation in *IDH*-mutated lines ($R = 0.12$; $P = 0.707$). Promoter methylation and mRNA expression were also negatively correlated in *IDH* wild-type lines but only marginally correlated in *IDH*-mutant lines ($R = 0.35$; $P = 0.27$). In contrast, body methylation and mRNA expression showed positive correlations in both *IDH* wild-type ($R = 0.7$; $P < 0.001$) and *IDH*-mutated lines ($R = 0.62$; $P = 0.033$). Regression models reinforced these findings; for *IDH* wild-type lines, both promoter and body methylation were significant predictors of mRNA expression (promoter $\beta = -3.1$; $P < 0.001$ and body $\beta = 0.89$; $P = 0.006$; Supplementary Table S1). However, for *IDH*-mutant lines, only body methylation remained significantly associated with mRNA expression (promoter $\beta = -3.87$; $P = 0.035$ and body $\beta = 3.29$; $P = 0.015$).

Response to carmustine in a glioma cell line panel

Carmustine was selected as the DNA-alkylating agent for testing a subset of the cell lines because of its stability at physiologic pH of cell culture media (1, 2) and because it does not require metabolic activation, which would complicate interpretation. Temozolomide, by comparison, is a prodrug that decomposes rapidly at physiologic pH, making it less reliable for consistent dosing in cell culture experiments (25). Eleven lines were chosen for testing their range of mRNA expression and promoter/body methylation (Fig. 3A and B), the high degree to which they recapitulated human disease as assessed by Molecular Neuropathology (MNP) methylation scores that approached one (Supplementary Table S2), and for range of genetic backgrounds. Three of the lines were *IDH* mutant (MGG119, GSC403, and TS603); one of which (TS603) also harbors

a chromosome 1p 19q co-deletion. U251 was included in panel because of its ubiquity as a glioma cell line model in preclinical studies, and NHA as a representative of normal human astrocytes. The MNP classifier categorized two cell lines, GSC274 and DIPG17, as having unmethylated *MGMT* promoters, whereas the remaining nine cell lines were classified as having methylated *MGMT* promoters (Supplementary Table S2). The response to carmustine varied, as shown by IC_{50} values (Fig. 4A), with lines categorized as sensitive ($IC_{50} < 45 \mu\text{mol/L}$), intermediate ($45 \mu\text{mol/L} < IC_{50} < 90 \mu\text{mol/L}$), or resistant ($IC_{50} > 90 \mu\text{mol/L}$). Resistant lines exhibited low promoter methylation, high body methylation, and low baseline protein production. Sensitive lines showed high promoter/body methylation and high baseline protein levels. Intermediate lines were a mix of non-expressing and variably expressing lines. Interestingly, DIPG17, which was expected to be more resistant based on the MNP classification, fell into the intermediate category, exhibiting a similar IC_{50} and body methylation status to the *MGMT* promoter-methylated, *IDH*-mutant line MGG119.

IC_{50} was positively correlated with gene body methylation ($R = 0.6$; $P = 0.05$) and mRNA expression ($R = 0.61$; $P = 0.04$), whereas negatively correlated with promoter methylation ($R = -0.72$; $P = 0.01$; Fig. 4C). Linear regression with an interaction term confirmed these associations (promoter $\beta = 728.7$; $P = 0.015$ and body $\beta = 685.65$, $P = 0.005$; interaction $P = 0.007$; Supplementary Table S1). Correlations and regression models evaluating the relationship between baseline protein levels and *MGMT* promoter methylation, body methylation, mRNA expression, or IC_{50} were statistically insignificant across all measures.

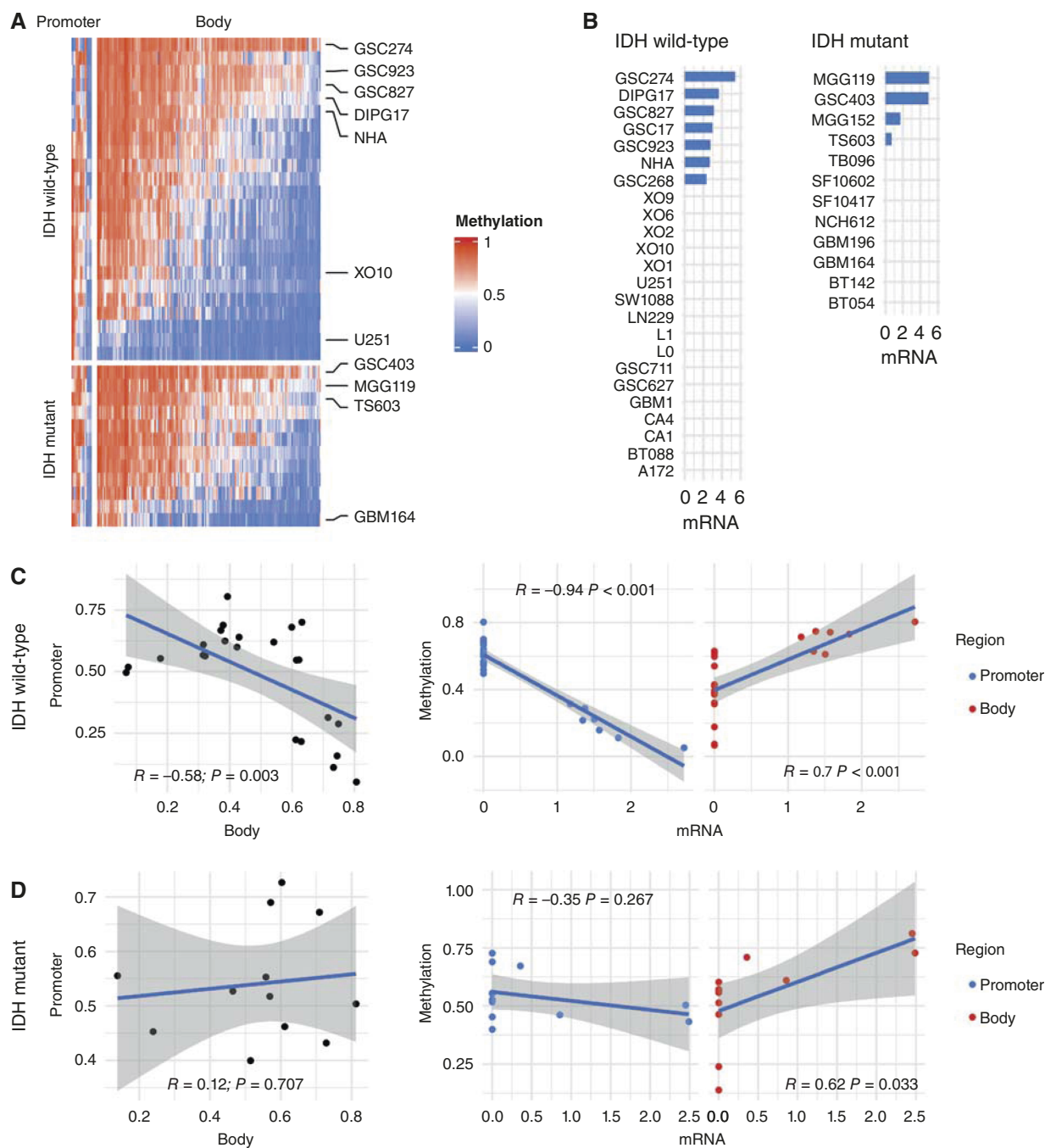
MGMT protein levels across passage, time, and carmustine dose

Poor correlation between *MGMT* baseline protein levels and other levels of *MGMT* regulation and carmustine response prompted further investigation. *MGMT* undergoes ubiquitination after binding O^6 methyl groups, leading to degradation. We hypothesized that the MT3.1 antibody detected only the free, non-ubiquitinated form of *MGMT*. Using an additional antibody (F-5) that binds both free and ubiquitinated *MGMT* (Fig. 5A) revealed extra bands, but none passed background levels for accurate quantification of total protein.

We also explored the possibility that *MGMT* production is dependent on cell line passage (Fig. 5B). Most cell lines showed stable levels although production for GSC923, a low-expressing line, dropped significantly from early to mid passage, whereas NHA and GSC274 peaked at mid passage. Using optimal passages, we then tested *MGMT* level response to increasing carmustine doses and exposure time at IC_{50} . As expected, higher doses reduced free protein levels. Over time at IC_{50} , most lines showed a decline in protein levels from 24 to 72 hours although GSC274 increased from 24 to 48 hours and plateaued at 72 hours, whereas MGG119 and GSC923 maintained stable levels. ANOVA results (Fig. 5B-D) confirmed decreasing protein levels with both time at IC_{50} and increasing carmustine doses.

Discussion

We assessed whether *MGMT* gene body methylation enhances the predictive accuracy of promoter methylation, which is commonly used as a marker for alkylating chemotherapy response in patients with glioma but is not entirely reliable. In a pan-cancer patient cohort, body methylation was positively correlated with *MGMT* mRNA expression,

**Figure 3.**

Methylation and gene expression of *MGMT* across human glioma cell lines and normal astrocytes, split by *IDH1/2* mutation status. **A**, Heatmaps displaying methylation probes (columns) from the promoter and body regions in various human cell lines (rows), profiled using methylation 850k arrays. Cell lines further tested for carmustine response and *MGMT* levels are labeled. **B**, Gene expression of *MGMT* in the same cell lines as measured by RNA sequencing, with the lines arranged in decreasing order of mRNA expression. **C** and **D**, Pearson correlations between aggregated methylation levels in the body and promoter regions, body methylation, and mRNA expression and promoter methylation and mRNA expression.

whereas promoter methylation was anticorrelated. This pattern was confirmed in a cell line panel, including gliomas and NHAs, although most lines expressed only low levels of *MGMT* mRNA. Testing a subset

for carmustine response, we found that response was significantly associated with promoter and body methylation, as well as mRNA expression, but showed no significant correlation with protein levels,

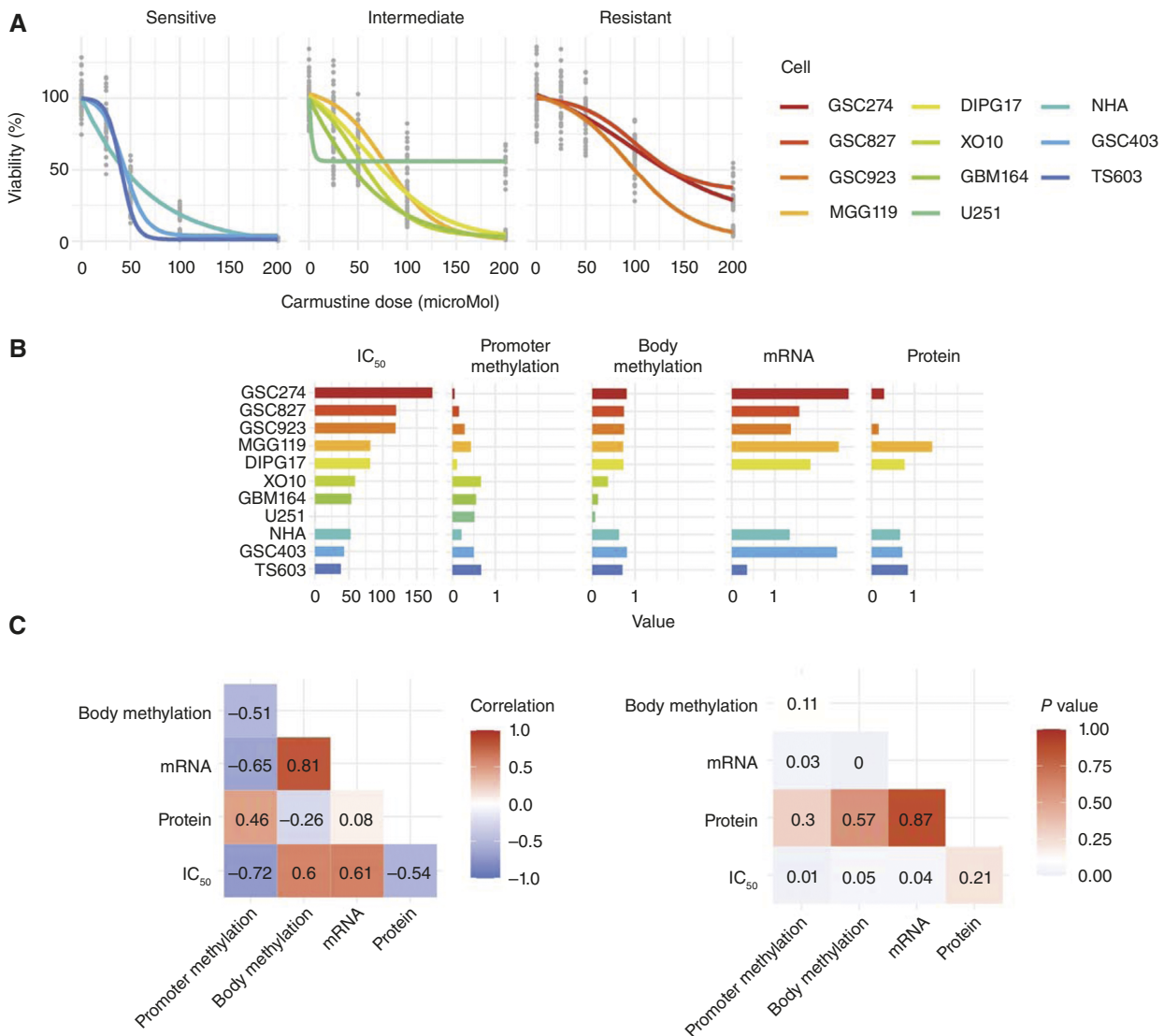


Figure 4.

Carmustine response and its correlation with *MGMT* methylation, expression, and protein levels. **A**, Carmustine response measured across increasing doses. **B**, Cell lines ranked by IC₅₀ values from most resistant to most sensitive, with corresponding levels of promoter methylation, body methylation, mRNA expression, and baseline protein levels. IC₅₀ for U251 could not be reliably determined. **C**, Pairwise Pearson correlations between IC₅₀, promoter methylation, body methylation, mRNA expression, and baseline protein levels, along with their respective *P* values.

whereas resistance was significantly associated with low promoter methylation and high gene body methylation.

Of note, *MGMT* levels detected by Western blotting showed poor correlation with the measured *MGMT* genetic regulatory levels. This inconsistency could stem from the low levels of *MGMT* in the glioma cancer cell lines as measured in the NCI-60 collection (Supplementary Fig. S1; refs. 26, 27), the sensitivity of the antibody used for detection, or the timing of protein collection. As a suicide protein, *MGMT* is degraded after use, and our analysis suggested that fast replenishment may contribute to resistance. Sensitive cell lines exhibited a steep decline in protein levels between 24 and 72 hours with no recovery, whereas lines with high body methylation but slightly lower promoter methylation likely had increased *MGMT* mRNA, supporting faster protein turnover.

Prior studies have underscored the importance of analyzing various *MGMT* genomic regions for DNA methylation determination (28–30). Additionally, *MGMT* methylation may change over the disease course, with tumors potentially losing promoter methylation upon recurrence (31, 32). Some studies have noted that *MGMT* protein levels do not always correlate with promoter methylation but can still inform survival outcomes when combined with other measures of regulatory regions (such as CpG 86 in exon 1 and the K-M enhancer; refs. 28, 30, 33, 34). Therefore, whole-gene methylation levels could provide a more precise determination of *MGMT* as a predictor.

Multiple probe amplification and sequencing-based assays are commonly used to detect methylation status, but these tests often show poor agreement, even on the same sample, due to variations in standards, cutoffs, methods of quantification, and regions assessed

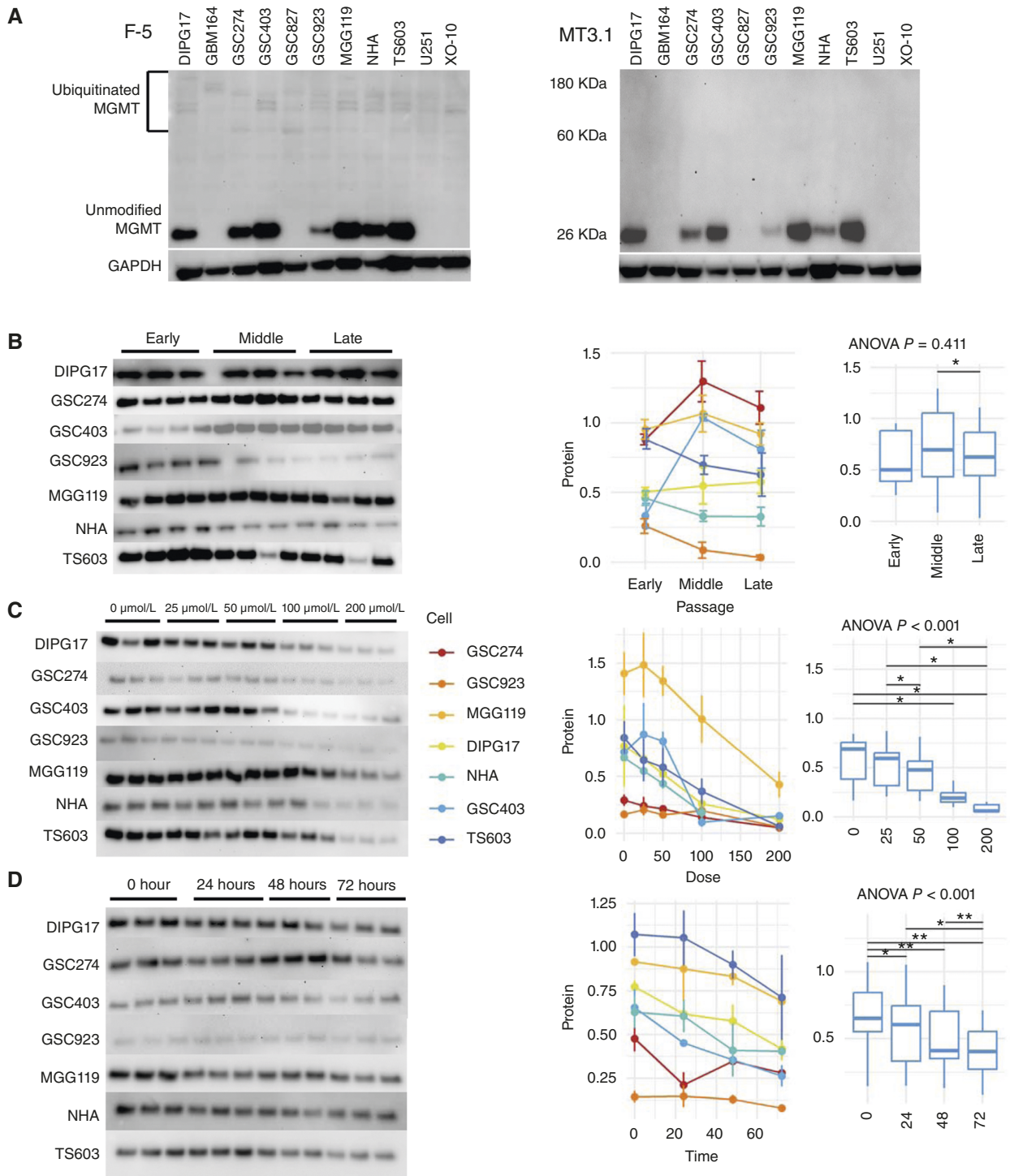


Figure 5.

MGMT quantification across passages, increasing carmustine doses, and over time with carmustine treatment. **A**, Western blotting using F-5 and MT3.1 antibodies for MGMT detection. **B**, Western blotting and quantification of MGMT protein levels across different passages. **C**, Quantification of MGMT levels after treatment with increasing carmustine concentrations for 48 hours. **D**, Time-dependent quantification of MGMT after treatment at IC_{50} concentrations. Statistical analyses were performed using ANOVA and paired t-tests (without adjustment for multiple comparisons), with outliers removed from all analyses.

(9). Chai and colleagues, for example, showed that CpG island sites used in commercial pyrosequencing testing exhibited heterogeneity of methylation levels, and that using separate cutoffs for individual

sites versus a single cutoff for the average methylation level refined prediction of response to temozolomide for patients with glioma (35, 36). The advent of nanopore sequencing technology offers a

novel approach, detecting epigenetic changes without modifying DNA, thereby avoiding errors typical of pyrosequencing and methylation bead assays (37). Its long-read capability allows the inclusion of distal enhancers, the full promoter, and the gene body in one analysis, enabling more comprehensive clinical testing. Alternatives like machine learning models using MRI or serum biomarkers have also been proposed to assess *MGMT* status although these approaches have limited accuracy or require multi-region analysis, which may not be feasible in all clinical settings (38–41).

IDH1/2 mutation status is likely important for the interpretation of results. In the *IDH1/2*-mutated glioma cohorts, promoter and body methylation were not significantly correlated, a relationship likely affected by the genome-wide hypermethylation caused by the production of D-2-hydroxyglutarate from neomorphic *IDH1/2* enzymes (42). The significant correlation between body methylation and mRNA expression, regardless of *IDH1/2* mutation status, underscores the potential importance of body methylation as a valuable factor in *MGMT* evaluation. Interestingly, cell line responses to treatment did not clearly divide by *IDH1/2* mutation status despite it being a strong survival predictor in patients. The relationship between *IDH1/2* mutation and *MGMT* remains unclear, with studies showing conflicting results on whether they are correlated or independent predictors of response (43–46). Chai and colleagues (43) found that predicting the therapeutic response to temozolomide in *IDH1/2* high-grade gliomas requires higher cutoffs for *MGMT* promoter methylation compared with *IDH1/2* wild-type gliomas.

Further complicating interpretation, gliomas frequently exhibit loss of heterozygosity on chromosome 10, in which *MGMT* is located. This loss could result in misclassifying samples as lacking sufficient promoter methylation, potentially overlooking patients who might respond to therapy. Most clinical tests do not account for this chromosomal loss, and incorporating this factor could enhance prediction accuracy.

Although the experimental studies were limited to *in vitro* cell line models, our focus panel was carefully selected to closely recapitulate human disease. High classification scores by the MNP classifier indicate the molecular similarity of these lines to human glioma subtypes and the panel included both *IDH1*-mutant and wild-type lines. However, these models cannot fully replicate the tumor microenvironment, a limitation also present in mouse-based animal models that do not mimic the immune microenvironment and the anatomy of human tumors. The inclusion of both *IDH1*-mutant and wild-type lines also constrained our ability to perform in-depth functional enrichment analyses. Comparing the transcriptomic profiles of carmustine-sensitive and carmustine-resistant tumor lines revealed broad enrichment for cancer-relevant pathways (Supplementary Fig. S2), but the diverse molecular backgrounds and small sample size made it challenging to formulate a clear hypothesis.

Carmustine was selected as the DNA-alkylating agent for testing because of its stability at non-acidic pH; temozolomide, by comparison, is a prodrug that decomposes rapidly at physiologic pH, making it less reliable for consistent dosing in cell culture experiments (25). Although their mechanism of action is similar in that both drugs are alkylating agents that cause DNA damage leading to cell death, temozolomide is more clinically relevant in the treatment of gliomas due to its delivery: temozolomide is administered systemically (orally or intravenously) whereas carmustine is primarily delivered locally via Gliadel wafers. The systemic administration of temozolomide is well tolerated, whereas systemic (intravenous) administration of carmustine is associated with significant systemic toxicities, including myelosuppression, hepatotoxicity, and pulmonary toxicity (47). Nevertheless, the American Society of Clinical Oncology and the

Society for Neuro-Oncology guidelines suggest that carmustine can be used as an adjuvant therapy to surgery and radiotherapy for newly diagnosed high-grade gliomas, including GBM, as implantation of the wafers in the resection cavity during surgery allows for high local concentrations of the drug while minimizing systemic toxicity (48). Clinical relevance and benefit of carmustine in the treatment of recurrent high-grade glioma have also been recognized (49, 50).

Conclusions

Our study adds to the growing body of evidence that *MGMT* expression and modulation of response to alkylating chemotherapy are multifactorial processes, with gene body methylation playing a significant role. Although *MGMT* promoter methylation is a well-established marker for predicting chemotherapy response in patients with glioma, our findings suggest that *MGMT* gene body methylation enhances the predictive power by positively correlating with mRNA expression and negatively with treatment sensitivity. This multifaceted regulation challenges the current clinical practice of relying solely on promoter methylation and underscores the need for a more comprehensive assessment of *MGMT* methylation patterns.

Clinically, incorporating gene body methylation into routine *MGMT* testing could lead to more accurate predictions of chemotherapy response, especially in patients with ambiguous promoter methylation results. Moreover, our findings point to the importance of considering factors like *MGMT* protein turnover and dynamics over time as they may influence resistance mechanisms. Integrating these insights into clinical practice could refine patient stratification for alkylating therapies, potentially improving survival outcomes. The complex interplay between *MGMT* body methylation, *IDH1/2* mutation status, and chromosomal abnormalities — particularly the loss of chromosome 10 in GBM — further complicates treatment response predictions. This underscores the need for optimizing *MGMT* testing to personalize therapeutic strategies in glioma management.

Authors' Disclosures

No disclosures were reported.

Authors' Contributions

N.J. Briceno: Formal analysis, investigation, methodology, writing—original draft, writing—review and editing. **J. Jung:** Resources, data curation, investigation, methodology, writing—review and editing. **A. Li:** Data curation, formal analysis, writing—review and editing. **C. Yang:** Resources, writing—review and editing. **M. Larion:** Resources, writing—review and editing. **L.S. Pongor:** Methodology, writing—review and editing. **F. Elloumi:** Conceptualization, methodology, writing—review and editing. **S. Varma:** Methodology. **W.C. Reinhold:** Conceptualization, supervision, methodology, writing—review and editing. **Y. Pommier:** Conceptualization, supervision, funding acquisition, visualization, methodology, writing—review and editing. **M.R. Gilbert:** Conceptualization, resources, supervision, funding acquisition, methodology, writing—review and editing. **O. Celiku:** Data curation, formal analysis, supervision, visualization, methodology, writing—original draft, writing—review and editing.

Acknowledgments

This work was supported by the Intramural Research Program of the NCI, NIH (Z01 BC 006150, ZIA BC 011684, and ZIA BC 011707).

Note

Supplementary data for this article are available at Molecular Cancer Therapeutics Online (<http://mct.aacrjournals.org/>).

Received October 29, 2024; revised February 28, 2025; accepted May 29, 2025; posted first June 4, 2025.

References

- Stevens MFG. Chapter 5 - temozolomide: from cytotoxic to molecularly targeted agent. In: Neidle S, editor. *Cancer drug design and discovery*. 2nd Ed. San Diego (CA): Academic Press; 2014. p. 145–64.
- Elgemeie GH, Mohamed-Ezzat RA. Chapter 8 - anticancer alkylating agents. In: Elgemeie GH, Mohamed-Ezzat RA, editors. *New strategies targeting cancer metabolism*. Amsterdam (the Netherlands): Elsevier; 2022. p. 393–505.
- Thomas A, Tanaka M, Trepel J, Reinhold WC, Rajapakse VN, Pommier Y. Temozolomide in the era of precision medicine. *Cancer Res* 2017;77:823–6.
- Hegi ME, Diserens A-C, Gorlia T, Hamou M-F, de Tribolet N, Weller M, et al. MGMT gene silencing and benefit from temozolomide in glioblastoma. *N Engl J Med* 2005;352:997–1003.
- Leu S, von Felten S, Frank S, Vassella E, Vajtai I, Taylor E, et al. IDH/MGMT-driven molecular classification of low-grade glioma is a strong predictor for long-term survival. *Neuro Oncol* 2013;15:469–79.
- Butler M, Pongor L, Su Y-T, Xi L, Raffeld M, Quezado M, et al. MGMT status as a clinical biomarker in glioblastoma. *Trends Cancer* 2020;6:380–91.
- Poon MTC, Sudlow CLM, Figueroa JD, Brennan PM. Longer-term (≥ 2 years) survival in patients with glioblastoma in population-based studies pre- and post-2005: a systematic review and meta-analysis. *Sci Rep* 2020;10:11622.
- Egaña L, Auzmendi-Iriarte J, Andermatten J, Villanua J, Ruiz I, Elua-Pinin A, et al. Methylation of MGMT promoter does not predict response to temozolomide in patients with glioblastoma in Donostia Hospital. *Sci Rep* 2020;10:18445.
- Johannessen LE, Brandal P, Myklebust TÅ, Heim S, Micci F, Panagopoulos I. MGMT gene promoter methylation status - assessment of two pyrosequencing kits and three methylation-specific PCR methods for their predictive capacity in glioblastomas. *Cancer Genomics Proteomics* 2018;15:437–46.
- Uno M, Oba-Shinjo SM, Camargo AA, Moura RP, Aguiar PH de, Cabrera HN, et al. Correlation of MGMT promoter methylation status with gene and protein expression levels in glioblastoma. *Clinics (Sao Paulo)* 2011;66:1747–55.
- Krushkal J, Silvers T, Reinhold WC, Sonkin D, Vural S, Connelly J, et al. Epigenome-wide DNA methylation analysis of small cell lung cancer cell lines suggests potential chemotherapy targets. *Clin Epigenet* 2020;12:93.
- Wang Q, Xiong F, Wu G, Liu W, Chen J, Wang B, et al. Gene body methylation in cancer: molecular mechanisms and clinical applications. *Clin Epigenetics* 2022;14:154.
- Pongor LS, Tlemsani C, Elloumi F, Arakawa Y, Jo U, Gross JM, et al. Integrative epigenomic analyses of small cell lung cancer cells demonstrates the clinical translational relevance of gene body methylation. *iScience* 2022;25:105338.
- Tlemsani C, Pongor L, Elloumi F, Girard L, Huffman KE, Roper N, et al. SCLC-CellMiner: a resource for small cell lung cancer cell line genomics and pharmacology based on genomic signatures. *Cell Rep* 2020;33:108296.
- Tlemsani C, Heske CM, Elloumi F, Pongor L, Khandagale P, Varma S, et al. Sarcoma_CellminerCDB: a tool to interrogate the genomic and functional characteristics of a comprehensive collection of sarcoma cell lines. *iScience* 2024;27:109781.
- Pang Y, Li Q, Sergi Z, Yu G, Sang X, Kim O, et al. Exploiting the therapeutic vulnerability of IDH-mutant gliomas with zotiraciclib. *iScience* 2025;28:112283.
- Tateishi K, Wakimoto H, Iafraite AJ, Tanaka S, Loebel F, Lelic N, et al. Extreme vulnerability of IDH1 mutant cancers to NAD⁺ depletion. *Cancer Cell* 2015; 28:773–84.
- Pipelin documentation. [cited 2024 Jul 18]. Available from: <https://ccbr.github.io/pipelin-docs/>.
- Aryee MJ, Jaffe AE, Corrada-Bravo H, Ladd-Acosta C, Feinberg AP, Hansen KD, et al. Minfi: a flexible and comprehensive Bioconductor package for the analysis of Infinium DNA methylation microarrays. *Bioinformatics* 2014;30:1363–9.
- Capper D, Jones DTW, Sill M, Hovestadt V, Schrimpf D, Sturm D, et al. DNA methylation-based classification of central nervous system tumours. *Nature* 2018;555:469–74.
- Bady P, Delorenzi M, Hegi ME. Sensitivity analysis of the MGMT-STP27 model and impact of genetic and epigenetic context to predict the MGMT methylation status in gliomas and other tumors. *J Mol Diagn* 2016;18:350–61.
- Goldman MJ, Craft B, Hastie M, McDade F, Kamath A, Banerjee A, et al. Visualizing and interpreting cancer genomics data via the Xena platform. *Nat Biotechnol* 2020;38:675–8.
- R Core Team. R: a language and environment for statistical computing. Vienna (Austria): R Foundation for Statistical Computing; 2013.
- Amatu A, Sartore-Bianchi A, Moutinho C, Belotti A, Bencardino K, Chirico G, et al. Promoter CpG island hypermethylation of the DNA repair enzyme MGMT predicts clinical response to dacarbazine in a phase II study for metastatic colorectal cancer. *Clin Cancer Res* 2013;19:2265–72.
- Lee SY. Temozolomide resistance in glioblastoma multiforme. *Genes Dis* 2016; 3:198–210.
- Reinhold WC, Varma S, Sunshine M, Rajapakse V, Luna A, Kohn KW, et al. The NCI-60 methylome and its integration into CellMiner. *Cancer Res* 2017; 77:601–12.
- Luna A, Elloumi F, Varma S, Wang Y, Rajapakse VN, Aladjem MI, et al. CellMiner Cross-Database (CellMinerCDB) version 1.2: exploration of patient-derived cancer cell line pharmacogenomics. *Nucleic Acids Res* 2021;49: D1083–93.
- Leske H, Camenisch Gross U, Hofer S, Neidert MC, Leske S, Weller M, et al. MGMT methylation pattern of long-term and short-term survivors of glioblastoma reveals CpGs of the enhancer region to be of high prognostic value. *Acta Neuropathol Commun* 2023;11:139.
- Brawanski KR, Sprung S, Freyschlag CF, Hoeflberger R, Ströbel T, Haybaeck J, et al. Influence of MMR, MGMT promoter methylation and protein expression on overall and progression-free survival in primary glioblastoma patients treated with temozolomide. *Int J Mol Sci* 2023;24:6184.
- Zappe K, Pühringer K, Pflug S, Berger D, Böhm A, Spiegel-Kreinecker S, et al. Association between MGMT enhancer methylation and MGMT promoter methylation, MGMT protein expression, and overall survival in glioblastoma. *Cells* 2023;12:1639.
- Choi HJ, Choi SH, You S-H, Yoo R-E, Kang KM, Yun TJ, et al. MGMT promoter methylation status in initial and recurrent glioblastoma: correlation study with DWI and DSC PWI features. *AJNR Am J Neuroradiol* 2021;42: 853–60.
- Brandes AA, Franceschi E, Paccapelo A, Tallini G, De Biase D, Ghimenton C, et al. Role of MGMT methylation status at time of diagnosis and recurrence for patients with glioblastoma: clinical implications. *The Oncologist* 2017;22: 432–7.
- Chen X, Zhang M, Gan H, Wang H, Lee J-H, Fang D, et al. A novel enhancer regulates MGMT expression and promotes temozolomide resistance in glioblastoma. *Nat Commun* 2018;9:2949.
- Li M, Dong G, Zhang W, Ren X, Jiang H, Yang C, et al. Combining MGMT promoter pyrosequencing and protein expression to optimize prognosis stratification in glioblastoma. *Cancer Sci* 2021;112:3699–710.
- Chai R-C, Zhang K-N, Liu Y-Q, Wu F, Zhao Z, Wang K-Y, et al. Combinations of four or more CpGs methylation present equivalent predictive value for MGMT expression and temozolomide therapeutic prognosis in gliomas. *CNS Neurosci Ther* 2019;25:314–22.
- Chai R-C, Liu Y-Q, Zhang K-N, Wu F, Zhao Z, Wang K-Y, et al. A novel analytical model of MGMT methylation pyrosequencing offers improved predictive performance in patients with gliomas. *Mod Pathol* 2019;32:4–15.
- Halldorsson S, Nagymihaly RM, Patel A, Brandal P, Panagopoulos I, Leske H, et al. Accurate and comprehensive evaluation of O6-methylguanine-DNA methyltransferase promoter methylation by nanopore sequencing. *Neuropathol Appl Neurobiol* 2024;50:e12984.
- Tasci E, Shah Y, Jagasia S, Zhuge Y, Shephard J, Johnson MO, et al. MGMT ProfWise: unlocking a new application for combined feature selection and the rank-based weighting method to link MGMT methylation status to serum protein expression in patients with glioblastoma. *Int J Mol Sci* 2024;25:4082.
- Li L, Xiao F, Wang S, Kuang S, Li Z, Zhong Y, et al. Preoperative prediction of MGMT promoter methylation in glioblastoma based on multiregional and multi-sequence MRI radiomics analysis. *Sci Rep* 2024;14:16031.
- Doniselli FM, Pascuzzo R, Agrò M, Aquino D, Anghileri E, Farinotti M, et al. Development of a radiomic model for MGMT promoter methylation detection in glioblastoma using conventional MRI. *Int J Mol Sci* 2023;25:138.
- Sanada T, Kinoshita M, Sasaki T, Yamamoto S, Fujikawa S, Fukuyama S, et al. Prediction of MGMT promoter methylation status in glioblastoma by contrast-enhanced T1-weighted intensity image. *Neurooncol Adv* 2024;6: vdae016.
- Turcan S, Rohle D, Goenka A, Walsh LA, Fang F, Yilmaz E, et al. IDH1 mutation is sufficient to establish the glioma hypermethylator phenotype. *Nature* 2012;483:479–83.

43. Chai R, Li G, Liu Y, Zhang K, Zhao Z, Wu F, et al. Predictive value of MGMT promoter methylation on the survival of TMZ treated IDH-mutant glioblastoma. *Cancer Biol Med* 2021;18:271–82.
44. Pandith AA, Qasim I, Baba SM, Koul A, Zahoor W, Afroze D, et al. Favorable role of IDH 1/2 mutations aided with MGMT promoter gene methylation in the outcome of patients with malignant glioma. *Future Sci OA* 2020;7:FSO663.
45. Molenaar RJ, Verbaan D, Lamba S, Zanon C, Jeuken JWM, Boots-Sprenger SHE, et al. The combination of IDH1 mutations and MGMT methylation status predicts survival in glioblastoma better than either IDH1 or MGMT alone. *Neuro-Oncology* 2014;16:1263–73.
46. Kurdi M, Shafique Butt N, Baeesa S, Alghamdi B, Maghrabi Y, Bardeesi A, et al. The impact of IDH1 mutation and MGMT promoter methylation on recurrence-free interval in glioblastoma patients treated with radiotherapy and chemotherapeutic agents. *Pathol Oncol Res* 2021;27:1609778.
47. Lin SH, Kleinberg LR. Carmustine wafers: localized delivery of chemotherapeutic agents in CNS malignancies. *Expert Rev Anticancer Ther* 2008;8:343–59.
48. Mohile NA, Messersmith H, Gatson NT, Hottinger AF, Lassman A, Morton J, et al. Therapy for diffuse astrocytic and oligodendroglial tumors in adults: ASCO-SNO guideline. *JCO* 2022;40:403–26.
49. Champeaux-Depond C, Jecko V, Weller J, Constantinou P, Tuppin P, Metellus P. Recurrent high grade glioma surgery with carmustine wafers implantation: a long-term nationwide retrospective study. *J Neurooncol* 2023;162:343–52.
50. Weller M, van den Bent M, Preusser M, Le Rhun E, Tonn JC, Minniti G, et al. EANO guidelines on the diagnosis and treatment of diffuse gliomas of adulthood. *Nat Rev Clin Oncol* 2021;18:170–86.